Space Charge Effects

M. Ferrario, M. Migliorati, and L. Palumbo
INFN-LNF and University of Rome "La Sapienza"

Abstract

The space charge forces are those generated directly by the charge distribution, with the inclusion of the image charges and currents due to the interaction of the beam with a perfectly conducting smooth pipe. Space charge forces are responsible of several unwanted phenomena related to beam dynamics, such as energy loss, shift of the synchronous phase and frequency, shift of the betatron frequencies, and instabilities. We will discuss in this lecture the main feature of space charge effects in high energy storage rings as well as low energy linacs and transport lines.

1. Introduction

Charged particles moving in a linear or circular accelerator are guided, confined and accelerated by external electromagnetic (e.m.) fields. In particular, the electric field in RF cavities is responsible of acceleration, while the magnetic fields guide and focus the particles: the bending magnets are used for guiding the charges on the reference trajectory (orbit), the solenoids or quadrupoles for the transverse confinement, and the sextupoles for the chromaticity correction.

The particle motion is governed by the Lorentz force through the equation:

$$\frac{d\left(m_0 \gamma \vec{v}\right)}{dt} = \vec{F}^{ext} = e\left(\vec{E} + \vec{v} \times \vec{B}\right) \tag{1}$$

where m_0 is the rest mass, γ is the relativistic factor and $\vec{v}$ is the particle velocity. With the above equation we can in principle calculate the trajectory of the charge moving through any e.m. field.

The external forces $\vec{F}^{ext}$ used for the beam transport and expressed by eq. (1) do not depend on the beam current. In a real accelerator, however, there is another important source of e.m. fields to be considered, the beam itself, which, circulating inside the pipe, produces additional e.m. fields called "self-fields". These fields, which depend on the intensity of the beam current and on the charge distribution, perturb the external guiding fields.

The self-fields are responsible of several unwanted phenomena related to beam dynamics, such as energy loss, shift of the synchronous phase and frequency, shift of the betatron frequencies, and instabilities. It is customary to divide the study of self-fields in space charge fields and wakefields. The space charge forces are those generated directly by the charge distribution, with the inclusion of the image charges and currents due to the interaction of the beam with a perfectly conducting smooth pipe [1]. The wakefields are instead produced by the finite conductivity of the walls and by all geometric variation of the beam pipe (such as resonant devices and transitions of the beam pipe). A reference paper on the wakefields can be found in [2].

We will discuss in this lecture space charge effects only, which are actually a particular case of Coulomb interactions in a multi-particle system. The net effect of the Coulomb interaction in a multi-particle system can be in fact classified into two regimes [3]:

- *collisional regime*, dominated by binary collisions caused by close particle encounters i.e. single particle scattering

- *collective regime or space charge regime*, dominated by the self-field produced by the particle distribution which varies appreciably only over large distances compared to the average separation of the particles.

The collisional part of the total interaction force arises when a particle is scattered by its immediate neighbors. This force will cause small random displacements of the particle's trajectory and statistical fluctuations in the particle distribution as a whole, leading for example to intra-beam scattering effects in high-energy storage rings [4] (see also Touschek effect [5]). On the other hand space charge forces lead to collective behavior of the beam driving for example envelope oscillations, emittance and energy spread growth [6].

A measure for the relative importance of collisional versus collective effects in a beam is the Debye length: $\lambda_D = \sqrt{\dfrac{\varepsilon_o \gamma^2 k_B T}{e^2 n}}$, where n is the particle density and the transverse beam temperature T is defined as $k_B T = \gamma m_o \langle v_\perp^2 \rangle$, k_B being the Boltzmann constant [3]. If a test charge is placed inside the beam, the excess electric potential Φ_D set up by this charge is effectively screened off in a distance λ_D by charge redistribution in the beam as: $\Phi_D(\vec{r}) = \dfrac{C}{r} e^{-r/\lambda_D}$. This effect is well known from plasma physics as *Debye shielding* [7]. A charged particle beam in a particle accelerator can be viewed in fact as a non-neutral plasma [8] in which the smooth focusing channel replaces the restoring force produced by ions in a neutral plasma, see Fig. 1. Like in a neutral plasma collective behavior of the beam can be observed on length-scales much larger than the Debye length. It follows that if the Debye length is much smaller compared to the beam radius, collective effects due to the self fields of the beam will play a dominant role in driving the beam dynamics with respect to binary collisions.
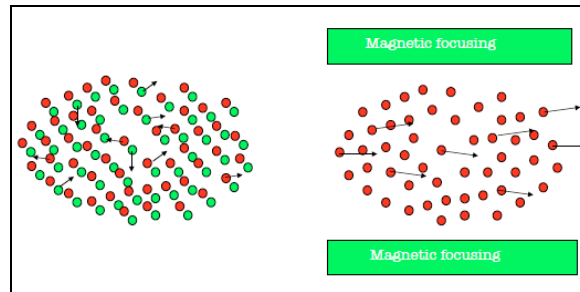

Fig. 1 – The restoring force produced by the ions (green dots) in a neutral plasma can be replaced by a smooth focusing channel for charged particle beam (non-neutral plasma) in a particle accelerator.

$$\Phi_D(\vec{r}) = \frac{C}{r} e^{-r/\lambda_D} \Rightarrow \begin{cases} \Phi_D(\vec{r}) \approx \Phi(\vec{r}) & \text{for } r << \lambda_D \\ \Phi_D(\vec{r}) << \Phi(\vec{r}) & \text{for } r \geq \lambda_D \end{cases}$$
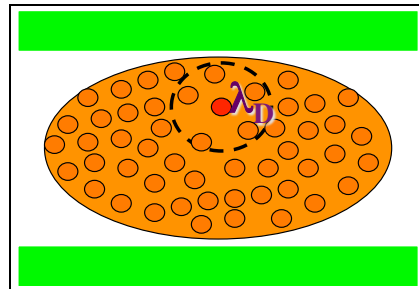

$$\Phi_{SC}(\vec{r}) \gg \Phi_D(\vec{r})$$

Fig. 2 –Representation of the Debye sphere surrounding a test particle (red) in a beam dominated by space charge smooth fields (uniform orange).

Smooth functions for the charge and field distributions can be used, as will be done in paragraph 3, as long as the Debye length remains large compared to the interparticle distance $d = n^{-1/3}$, that is as long as the number N_D of particles within a Debye sphere of radius λ_D remains large ($N_D \gg 1$). A typical particle is actually scattered by all of the other particles within its Debye sphere, but the large number of random interaction very rarely causes any sudden change in its motion (weakly coupled plasma) and mainly contribute in driving the beam toward a thermal equilibrium [3].

The smoothed space-charge forces acting on a particle can be thus treated like an external force and can be separated into linear and nonlinear terms as a function of displacement from the beam axis. The linear space-charge term typically defocuses the beam and leads to an increase in beam size. The nonlinear space-charge term increases the rms emittance by distorting the phase-space distribution. We shall see in paragraph 6 that also the linear component of the space charge field can induce reversible emittance growth in a bunched beam when longitudinal/transverse correlations along the bunch are taken in to account.

Notice that the Debye length increases with particle energy γ so that at sufficiently high energy a transition from space charge to collisional regime may occur.

2.   Self fields and equations of motion

2.1   The betatron motion

Before dealing with the self induced forces produced by the space charge and their effect on the beam dynamics in a circular accelerator, we briefly review the transverse equations of motion [9]. In order to simplify our study, let us consider a perfectly circular accelerator with radius ρ_x and obtain the transverse single particle equation of motion in the linear regime.

If we include, in the particle equation of motion given by eq. (1), the self induced forces, we have

$$\frac{d\left(m_0 \gamma \vec{v}\right)}{dt} = \vec{F}^{ext}\left(\vec{r}\right) + \vec{F}^{self}\left(\vec{r}\right) \tag{2}$$

By considering a constant energy γ it becomes:

$$\frac{d\vec{v}}{dt} = \frac{\vec{F}^{ext}\left(\vec{r}\right) + \vec{F}^{self}\left(\vec{r}\right)}{m_0 \gamma} \tag{3}$$
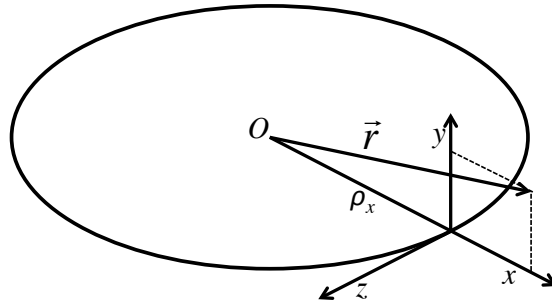

Fig. 3: Coordinate system for a charge in a circular accelerator.

According to the coordinate system of Fig. 3, indicating with $\vec{r}$ the charge position, and with x and y the transverse displacements with respect to the reference trajectory, we write:

$$\vec{r} = \left(\rho_x + x\right)\hat{e}_x + y\hat{e}_y \qquad (4)$$

Since the unit vector $\hat{e}_x$ rotates with angular frequency ω_0 (clockwise in the figure), its time derivative is $\omega_0 \hat{e}_z$, so that the velocity is

$$\vec{v} = \frac{d\vec{r}}{dt} = \dot{x}\hat{e}_x + \dot{y}\hat{e}_y + \omega_0\left(\rho_x + x\right)\hat{e}_z \qquad (5)$$

and the acceleration

$$\vec{a} = \left[\ddot{x} - \omega_0^2\left(\rho_x + x\right)\right]\hat{e}_x + \ddot{y}\hat{e}_y + \left[\dot{\omega}_0\left(\rho_x + x\right) + 2\omega_0\dot{x}\right]\hat{e}_z \qquad (6)$$

In the above equations the dots mean derivative with respect to time.

If we consider the motion along x, we have:

$$\ddot{x} - \omega_0^2\left(\rho_x + x\right) = \frac{1}{m_0\gamma}\left(F_x^{ext} + F_x^{self}\right) \qquad (7)$$

Instead of using the time t as variable, we consider the azimuthal position $s = v_z t$, so that the acceleration along x becomes

$$\ddot{x} = \frac{d^2 x}{dt^2} = v_z^2 \frac{d^2 x}{ds^2} = v_z^2 x'' = \omega_o^2\left(\rho_x + x\right)^2 x'' \qquad (8)$$

for which we have also used eq. (5). With the above equation, the differential equation of motion (7) can be written as

$$x'' - \frac{1}{\rho_x + x} = \frac{1}{m_0 v_z^2 \gamma}\left(F_x^{ext} + F_x^{self}\right) \qquad (9)$$

We assume now small transverse displacements x with respect to the machine radius ρ_x, so that we can linearly expand the above equation into

$$x'' - \frac{1}{\rho_x} + \frac{1}{\rho_x^2} x = \frac{1}{m_0 v_z^2 \gamma}\left(F_x^{ext} + F_x^{self}\right) \qquad (10)$$

In addition, we have that the external force is due to the magnetic guiding fields. We suppose to have only dipoles and quadrupoles, or, equivalently, we expand the external guiding fields in a Taylor series up to the quadrupole component

$$-F_x^{ext} = qv_z B_y = qv_z B_{y0} + qv_z \left(\frac{\partial B_y}{\partial x}\right)_0 x + \dots \qquad (11)$$

and recognize that the dipolar magnetic field B_{y0} is responsible of the circular motion along the reference trajectory of radius ρ_x according to the equation

$$qv_zB_{y0} = \frac{m_0\gamma v_z^2}{\rho_x} \tag{12}$$

We finally obtain

$$x'' + \left[\frac{1}{\rho_x^2} + \frac{q}{m_0 v_z \gamma}\left(\frac{\partial B_y}{\partial x}\right)\right]x = \frac{1}{m_0 v_z^2 \gamma}F_x^{self} \tag{13}$$

which can also be written as

$$x'' + \left[\frac{1}{\rho_x^2} - k\right]x = \frac{1}{m_0 v_z^2 \gamma}F_x^{self} \tag{14}$$

where we have introduced the normalized gradient

$$k = \frac{g}{p/q} = -\frac{q}{m_0 v_z \gamma}\left(\frac{\partial B_y}{\partial x}\right) \tag{15}$$

with g the quadrupole gradient in [T/m] and p the charge momentum.

Eq. (14) is not exactly correct, because both the curvature radius and the normalized gradient depend on the azimuthal position 's'. By using the focusing constant $K_x(s)$ we then should write

$$x''(s) + K_x(s)x(s) = \frac{1}{m_0 v_z^2 \gamma}F_x^{self}(x,s) \tag{16}$$

In absence of self fields, the solution of the free equation (Hill's equation) gives the well known betatron oscillations:

$$x(s) = a_x\sqrt{\beta_x(s)}\cos\left[\mu_x(s) - \varphi_x\right] \tag{17}$$

where a_x and φ_x depend on the initial conditions, and

$$\begin{aligned}
&\frac{1}{2}\beta_x\beta_x'' - \frac{1}{4}\beta_x'^2 + K_x(s)\beta_x^2 = 1 \\
&\mu_x'(s) = 1/\beta_x(s) \\
&Q_x = \frac{\omega_x}{\omega_o} = \frac{1}{2\pi}\int_0^L\frac{ds'}{\beta_x(s')}
\end{aligned} \tag{18}$$

with Q_x the betatron tune.

In the analysis of the motion in presence of the self induced fields, however, we adopt a simplified model where particles execute simple harmonic oscillations around the reference trajectory. This is equivalent to have the focusing term K_x constant around the machine. Although this case is never fulfilled in a real accelerator, however it provides a reliable model for the description of the beam instabilities. Under this approximation eq. (16) becomes

$$x''(s) + K_x x(s) = \frac{1}{m_0 v_z^2 \gamma}F_x^{self}(x,s) \tag{19}$$

which is a linear differential equation. The homogeneous solution is given by

$$x(s) = A_x \cos\left[\sqrt{K_x}s - \varphi_x\right]$$

(20)

were, with the notations of eq. (18), we have

$$a_x \sqrt{\beta_x} = A_x$$

$$\beta_x = \frac{1}{\mu'_x} = \frac{1}{\sqrt{K_x}}$$

$$\mu_x(s) = \sqrt{K_x}s$$

$$Q_x = \frac{1}{2\pi}\int_0^L \frac{ds'}{\beta_x(s')} = \frac{L}{2\pi\beta_x} = \rho_x\sqrt{K_x} \Rightarrow K_x = \left(\frac{Q_x}{\rho_x}\right)^2$$

(21)

The differential equation of motion (19) then becomes

$$x''(s) + \left(\frac{Q_x}{\rho_x}\right)^2 x(s) = \frac{1}{m_0 v_z^2 \gamma} F_x^{self}(x,s)$$

(22)

An analogous equation of motion can also be written for the vertical plane:

$$y''(s) + \left(\frac{Q_y}{\rho_x}\right)^2 y(s) = \frac{1}{m_0 v_z^2 \gamma} F_y^{self}(y,s)$$

(23)

Eqs. (22) and (23) represent our starting point to study the effects of the self induced fields on the betatron oscillations. Before analyzing such forces, let's write the analogous equation for the longitudinal dynamics.

2.2   The synchrotron motion

In the longitudinal case the motion is governed by the RF voltage, which we write as

$$V(t) = \hat{V} \sin\left[\omega_{rf}t + \varphi_s\right]$$

(24)

where φ_s is the synchronous phase. In the linear approximation, and in absence of the self induced forces, the equation of motion is that of a simple harmonic oscillator

$$z'' + \left(\frac{Q_z}{\rho_x}\right)^2 z = 0$$

(25)

with particles oscillating around the synchronous phase φ_s with a synchronous tune given by:

$$Q_z = \frac{\omega_z}{\omega_0} = \sqrt{\frac{qh\eta\hat{V}\cos\varphi_s}{2\pi\beta^2 E_0}}$$

(26)

with h the harmonic number, E_0 the machine nominal energy, and

$$\eta = \frac{1}{\gamma^2} - \alpha_c$$

(27)

The slippage factor η accounts for the increase of the speed with energy $(1/\gamma^2)$, and the length of the real orbit due to the dispersion (α_c).

The interaction of the charge with the surroundings may induce longitudinal e.m. forces, which have to be included in the equation of motion:

$$z'' + \left(\frac{Q_z}{\rho_x}\right)^2 z = \frac{\eta \, F_z^{self}(s)}{m_0 v_z^2 \gamma} \tag{28}$$

In the linear approximation, the longitudinal force produces a shift of both the synchronous phase and the synchronous tune.

3. Space charge forces

3.1 Direct space charge forces in the free space

Let us consider a relativistic charge moving with constant velocity $\vec{v}$. It is well known that its electrostatic field is modified because of the relativistic Lorentz contraction along the direction of motion as shown in Fig. 4. For an ultra-relativistic charge with $\gamma \rightarrow \infty$, the field lines are confined on a plane perpendicular to the direction of motion.
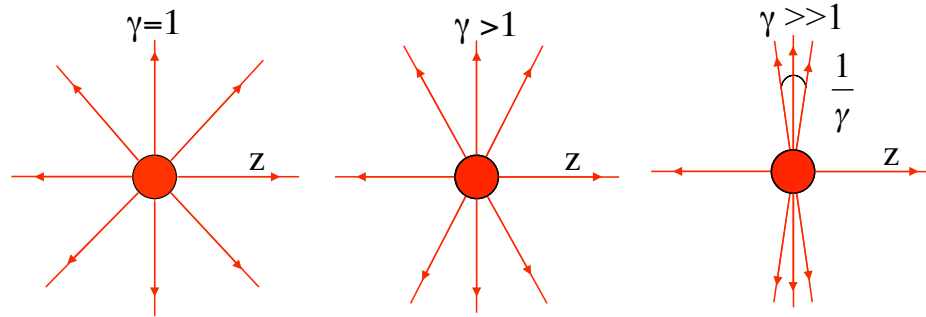

Fig. 4: Field lines for charges at different energies.

If now another charge is travelling on a parallel trajectory with respect to the first one along the z axis, it is easy to see that the e.m. forces between them vanish. In fact, from the relativistic transforms of the electric and magnetic fields of a point charge, by using a cylindrical coordinate system (r, ϕ, z) with the origin in the source charge, we have

$$E_r(z = 0) = \frac{q}{4\pi \, \varepsilon_0} \frac{\gamma}{r^2}$$

$$B_\phi(z = 0) = \frac{q\beta}{4\pi\varepsilon_0 c} \frac{\gamma}{r^2} \tag{29}$$

$$E_z(r = 0) = \frac{q}{4\pi \, \varepsilon_0} \frac{1}{\gamma^2 z^2}$$

If the two charges travel along the z axis at $r = 0$ with different longitudinal positions, then the force is proportional to the longitudinal electric field E_z, and it vanishes as $1/\gamma^2$. On the other hand, if the charges have the same longitudinal position $(z = 0)$ and different transverse position, due to the combined effect of the defocusing electric and focusing magnetic fields we get

$$F_r = q\left(E_r - \beta c B_\phi\right) = \frac{q\gamma}{4\pi\varepsilon_0 r^2}\left(1 - \beta^2\right) = \frac{q}{4\pi\varepsilon_0\gamma}\frac{1}{r^2} \tag{30}$$

In both cases, for $\gamma\to\infty$, a charge travelling close to another one on a parallel trajectory is not affected by e.m. forces.

Let us now consider the case of a uniform cylindrical charge distribution travelling with ultra-relativistic speed in the free space. Under these assumptions, the electric field lines are perpendicular to the direction of motion, and the magnetic ones are circumferences, as shown in Fig. 5. The transverse electric and magnetic fields intensity can be computed as in the static case, applying the Gauss and Ampere laws:

$$\int_S \vec{E}\cdot\hat{n}\,dS = \frac{q}{\varepsilon_0}, \qquad \oint_l \vec{B}\cdot d\vec{l} = \mu_0 I \tag{31}$$

We now suppose that the beam is a uniform cylinder of radius a so that the longitudinal charge distribution (charge per unit of length) can be written as $\lambda(r) = \lambda_o\left(\dfrac{r}{a}\right)^2$, and we want to compute the transverse space charge forces acting on a particle inside the beam.

Applying eqs. (31) to a cylinder for the Gauss's law and to a circumference for the Ampere's law we obtain:

$$
\begin{aligned}
E_r(2\pi r)\Delta z &= \frac{\lambda(r)\Delta z}{\varepsilon_0} \Rightarrow E_r = \frac{\lambda(r)}{2\pi\varepsilon_0 r} = \frac{\lambda_0}{2\pi\varepsilon_0}\frac{r}{a^2} \\
2\pi r B_\phi &= \mu_0 J\pi r^2 = \mu_0\beta c\lambda(r) \Rightarrow B_\phi = \frac{\lambda_o\beta}{2\pi\varepsilon_0 c}\frac{r}{a^2}
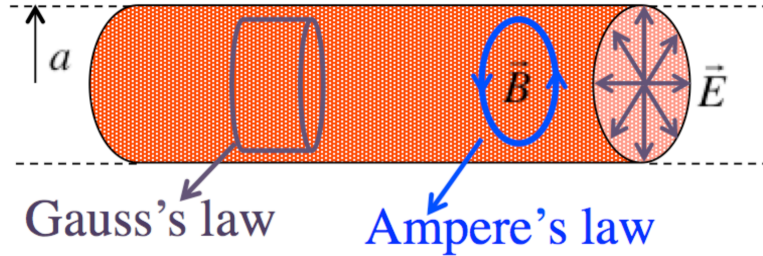\end{aligned}
\tag{32}
$$

Fig. 5: Uniform cylindrical charge distribution with its electric and magnetic fields.

We now observe that $B_\phi = \dfrac{\beta}{c}E_r$, so that the e.m. transverse force acting on a charge inside the beam is

$$F_r(r) = e(E_r - \beta c B_\phi) = e(1 - \beta^2)E_r = \frac{e}{\gamma^2}\frac{\lambda_o}{2\pi\varepsilon_0}\frac{r}{a^2} \tag{33}$$

We can therefore conclude that inside a uniform cylindrical charge density, travelling with ultra-relativistic speed, the transverse space charge forces vanish as $1/\gamma^2$ due to the cancellation of the electric and the magnetic forces.

3.2 Effects of conducting and magnetic screens

In an accelerator, the beams travel inside a vacuum pipe generally made of metallic material (as aluminum, copper, stainless steel). This pipe also passes through the coils of magnets (dipoles, quadrupoles, sextupoles), and its cross section may have a complicated shape, as in the case of special devices like RF cavities, kickers, diagnostics and controls. However, most part of the beam pipe has a cross section with a simple shape: circular, elliptic or quasi-rectangular. In order to obtain the space charge forces acting on a beam, let us consider only a smooth beam pipe perfectly conducting.

Before dealing with the problem, it is first necessary to review the basic features of e.m. fields close to metallic and magnetic materials. A discussion of the boundary conditions is given in the Appendix 1. Here we report only the more relevant conclusions. The electric field of a point charge close to a conducting screen can be derived through the method of images, as shown in Fig. A1. For what concerns the magnetic field, a constant current close to a good conductor screen with $\mu_r \approx 1$, as copper or aluminium, produces circular field lines not affected by the presence of the material itself. However, if the material is of ferromagnetic type, with $\mu_r >> 1$, due to its magnetisation, the magnetic field lines are strongly affected, inside and outside the material. In particular a very high magnetic permeability makes the tangential field zero at the boundary so that the total magnetic field must perpendicular to the surface, just like the electric field lines close to a conductor (see Fig. A2).

As discussed in Appendix 1, the scenario changes when we deal with time-varying fields for which it is necessary to compare the wall thickness and the skin depth (region of penetration of the e.m. fields) in the conductor. If the fields penetrate and pass through the material, we are practically in the static boundary conditions case. Conversely, if the skin depth is very small, fields do not penetrate, and then the electric filed lines are perpendicular to the wall, as in the static case, while the magnetic field lines are tangent to the surface. In this case, the magnetic field lines can be obtained by considering two currents flowing in opposite directions.

In the following paragraphs we analyse the forces due to the presence of the screens in some simple cases.

3.3 Circular perfectly conducting pipe with beam at center and direct space charge forces

Due to the symmetry, the transverse fields produced by an ultra-relativistic charge inside a circular, perfectly conducting pipe are the same as in the free space. This implies that for a charge distribution with cylindrical symmetry, in ultra-relativistic regime, the total force acting on a charge inside the beam is still given by eq. (33). It is interesting to note that this result does not depend on the longitudinal distribution of the beam, so that, considering more generally a uniform radial distribution and a longitudinal linear density $\lambda(z)$, the force is

$$F_r(r,z) = \frac{e}{\gamma^2} \frac{\lambda(z)}{2\pi\varepsilon_0} \frac{r}{a^2} \tag{34}$$

This force, as that in the free space, has a dependence that goes as $1/\gamma^2$ due to the cancellation of the electric and magnetic forces, and it is linear with the transverse position r. If the transverse distribution is not constant, we can still apply the Gauss's law to obtain the electric field and the Ampere's law to obtain the magnetic field. For example, given the following distribution:

$$\rho(r,z) = \frac{q_0}{\left(\sqrt{2\pi}\right)^3 \sigma_z \sigma_r^2} e^{\frac{-z^2}{2\sigma_z^2}} e^{\frac{-r^2}{2\sigma_r^2}} \tag{35}$$

with q_0 the bunch charge, the Gauss's law applied to a cylinder as that of Fig. 5 with an infinitesimal height dz, gives, as radial electric field (we suppose $\gamma \rightarrow \infty$ so that $E_z \approx 0$),

$$E_r(r,z) = \frac{1}{2\pi\varepsilon_0} \frac{q_0}{\sqrt{2\pi}\sigma_z\sigma_r^2 r} e^{\frac{-z^2}{2\sigma_z^2}} \int_0^r e^{\frac{-r^2}{2\sigma_r^2}} r' dr' = \frac{1}{2\pi\varepsilon_0} \frac{q_0}{\sqrt{2\pi}\sigma_z} e^{\frac{-z^2}{2\sigma_z^2}} \left[\frac{1 - e^{\frac{-r^2}{2\sigma_r^2}}}{r} \right] \tag{36}$$

The magnetic field can be obtained in the same way as in eq. (32) so that the total force on a charge inside the bunch is

$$F_r(r,z) = e(1-\beta^2)E_r = \frac{e}{2\pi\varepsilon_0\gamma^2} \frac{q_0}{\sqrt{2\pi}\sigma_z} e^{\frac{-z^2}{2\sigma_z^2}} \left[\frac{1 - e^{\frac{-r^2}{2\sigma_r^2}}}{r} \right] \tag{37}$$

It is important to observe that the self induced forces given by eqs. (34) and (37) are always defocusing either in x and in y direction, as shown in Fig. 6. Note that the force given by eq. (37) is not linear in the transverse position.
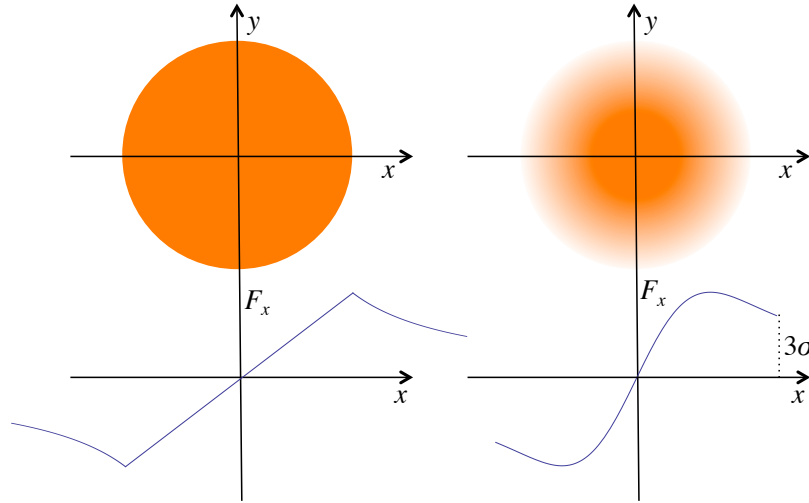

Fig. 6: Defocusing transverse self induced forces produced by direct space charge in case of uniform (left) and Gaussian (right) distributions.

3.4 Parallel plates with beam at center and indirect space charge forces for d.c. currents

In some cases, also with elliptical beam pipe, the cross section is such that we can consider only the surfaces closer to the beam, which can be approximated by two parallel plates. Let us suppose to have a charge distribution $\lambda(z)$ of radius a between two conducting plates $2h$ apart. For obtaining the static electric field, the two conducting plates can be removed by using the method of images and substituted by an infinite series of charges with alternating sign $2h$ apart each other, as shown in Fig. 7.

We now want to evaluate the electric field, due to the image charges, at a position y inside the bunch ($y<a$). The transverse field of the image charge distribution immediately above the real one can be written as

$$E_y^{1,up,im}(z,y) = \frac{\lambda(z)}{2\pi \ \varepsilon_0} \frac{1}{2h-y} \tag{38}$$

while the transverse electric field of the image charge distribution immediately below the real one is,

$$E_y^{1,down,im}(z,y) = -\frac{\lambda(z)}{2\pi \ \varepsilon_0}\frac{1}{2h+y} \tag{39}$$
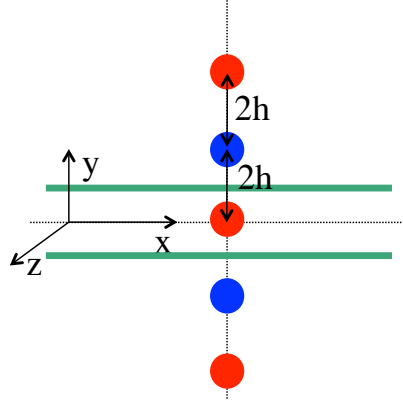

Fig. 7: A charge between two parallel plates and its image charges.

If we sum the contribution of all the infinite image charge distributions, we get the total transverse electric field

$$E_y^{im}(z,y) = \frac{\lambda(z)}{2\pi \ \varepsilon_0}\sum_{n=1}^{\infty}(-1)^n\left[\frac{1}{2nh+y}-\frac{1}{2nh-y}\right] = \frac{\lambda(z)}{2\pi \ \varepsilon_0}2y\sum_{n=1}^{\infty}(-1)^{n+1}\frac{1}{(2nh)^2-y^2} \tag{40}$$

The sum on the right hand side can be done. We consider however the simplified hypothesis that $h \gg a \gg y$, so we can ignore the term y in the denominator of the sum and we get

$$E_y^{im}(z,y) \cong \frac{\lambda(z)}{2\pi \ \varepsilon_0}\frac{y}{2h^2}\sum_{n=1}^{\infty}\frac{(-1)^{n+1}}{n^2} = \frac{\lambda \ (z)}{4\pi \ \varepsilon_0 h^2}\frac{\pi^2}{12}y \tag{41}$$

For d.c. or slowly varying currents, we have seen that the boundary conditions imposed by the conducting plates do not affect the magnetic field, which remains circular with no image currents. As a consequence there is no cancellation effect of the electric and magnetic forces for the fields produced by the images, as we have obtained for the real charges (direct forces), and the indirect force acting on a charge inside the beam is simply the electric field (41) times the particle charge.

From the divergence equation, we derive also the other transverse component of the electric field along x

$$\frac{\partial}{\partial x}E_x^{im} = -\frac{\partial}{\partial y}E_y^{im} \Rightarrow E_x^{im}(z,x) = \frac{-\lambda(z)}{4\pi \ \varepsilon_0 h^2}\frac{\pi^2}{12}x \tag{42}$$

From the above fields, the total forces acting on a charge inside the bunch moving between two parallel plates, including also the direct space charge force given by eq. (34), are:

$$F_x(z,x) = \frac{e\lambda(z)}{\pi \ \varepsilon_0}\left(\frac{1}{2a^2\gamma^2}-\frac{\pi^2}{48h^2}\right)x \tag{43}$$

$$F_y(z,y) = \frac{e\lambda(z)}{\pi \ \varepsilon_0}\left(\frac{1}{2a^2\gamma^2}+\frac{\pi^2}{48h^2}\right)y \tag{44}$$

Therefore, for $\gamma \gg 1$, and for d.c. or slowly varying currents, the cancellation effect applies only to the direct space charge forces. There is no cancellation of the electric and magnetic forces due to the image charges.

3.5 Parallel plates with beam at center and indirect space charge forces for a.c. currents

We have seen that close to a conductor the e.m. fields have different behaviours, depending on the skin depth δ_w of the material (Appendix 1). Usually, the frequency spectrum of a beam is quite rich of harmonics, especially for bunched beams. It is then convenient to decompose the current into a d.c. component, $\bar{I}$, for which $\delta_w \gg \Delta w$, with Δw the width of the beam pipe, and an a.c. component, $\hat{I}$, for which $\delta_w \ll \Delta w$. While the d.c. component of the magnetic field does not perceives the presence of the material, so that we can apply eqs. (43) and (44), its a.c. component produces a magnetic field tangent to the wall, which can be obtained by using an infinite sum of image currents with alternating directions. In this case, to get the total magnetic field of the image currents, we can follow the same procedure we have used for the electric fields given by eqs. (41) and (42), and by considering the relation between a.c. current and its charge distribution: $\hat{I} = \beta c \hat{\lambda}$, thus obtaining a magnetic field due to image currents of the kind

$$\hat{B}_x(z,y) = -\frac{\beta}{c}\hat{E}_y(z,y) = -\frac{\beta^2\hat{\lambda}(z)}{\pi\,\varepsilon_0}\frac{\pi^2}{48h^2}y; \tag{45}$$

We can see from the above expression that in this case the attractive magnetic force tends to compensate the repulsive electric one, which is still given by the second term in the parentheses of eq. (44), so that we have a total force due to image charges and currents given by

$$\hat{F}_y(z,y) = \frac{e\hat{\lambda}(z)}{\pi\,\varepsilon_o\gamma^2}\frac{\pi^2}{48h^2}y \tag{46}$$

Combining eq. (46) with the direct space charge force, we get for the a.c. component:

$$\hat{F}_y(z,y) = \frac{e\hat{\lambda}(z)}{2\pi\,\varepsilon_0\gamma^2}\left(\frac{1}{a^2} + \frac{\pi^2}{24h^2}\right)y \tag{47}$$

and analogously along the x direction

$$\hat{F}_x(z,x) = \frac{e\hat{\lambda}(z)}{2\pi\,\varepsilon_0\gamma^2}\left(\frac{1}{a^2} - \frac{\pi^2}{24h^2}\right)x \tag{48}$$

3.6 Parallel plates with beam at center and indirect space charge forces for d.c. currents in presence of ferromagnetic materials

As a last example we consider now the case where outside of the metallic pipe there is a dipole magnet. The magnetic field produced by the d.c. currents $\beta c\bar{\lambda}(z)$ doesn't see the conducting pipe, while it is strongly affected by ferromagnetic material. In fact, as seen in the Appendix 1, the magnetic field lines must be orthogonal to the pole surface. We have also seen that the total magnetic field can be obtained by removing the screen and considering image currents flowing in the same direction.

Proceeding analogously to Sec. 3.4, with g the gap in the dipole magnet, we obtain:

$$B_x^{im}(z,y) = \frac{\mu_0\beta c\bar{\lambda}(z)}{2\pi}\sum_{n=1}^{\infty}\left[\frac{1}{2ng-y} - \frac{1}{2ng+y}\right] \tag{49}$$

Note that in this case we don't have the term $(-1)^n$. By using the same approximation as before $h \gg a > y$, we obtain a magnetic field due to the image currents equal to

$$B_x^{im}(z,y) \cong \frac{\mu_0 \beta c \bar{\lambda}(z) y}{4 \pi g^2} \sum_{n=1}^{\infty} \frac{1}{n^2} = \frac{\mu_0 \beta c \bar{\lambda}(z) \pi^2 y}{24 \pi g^2} \tag{50}$$

and the corresponding force is

$$F_y^{im}(z,y) = \frac{\beta^2 \bar{\lambda}(z) \pi^2}{24 \pi \varepsilon_0 g^2} y \tag{51}$$

In order to obtain the magnetic field acting on a particle displaced along the x direction, we can use the relation $\vec{\nabla} \times \vec{B} = 0$, which, for the z direction gives

$$\frac{\partial B_y}{\partial x} = \frac{\partial B_x}{\partial y} \tag{52}$$

so that

$$B_y^{im}(z,x) = \frac{\mu_0 \beta c \bar{\lambda}(z) \pi^2}{24 \pi g^2} x \tag{53}$$

and

$$F_x^{im}(z,x) = -\frac{\beta^2 \bar{\lambda}(z) \pi^2}{24 \pi \varepsilon_0 g^2} x \tag{54}$$

3.7 Parallel plates with beam at center: general expression of the force

Taking into account all the boundary conditions and either d.c. and a.c. currents, we can summarize what we have obtained in the previous sections for the parallel plates, and write the general expression of the force as:

$$F_u = \frac{e}{2\pi \ \varepsilon_0} \left[\frac{1}{\gamma^2} \left(\frac{1}{a^2} \mp \frac{\pi^2}{24h^2} \right) \lambda \mp \beta^2 \left(\frac{\pi^2}{24h^2} + \frac{\pi^2}{12g^2} \right) \bar{\lambda} \right] u \tag{55}$$

where λ is the total current divided by βc, and $\bar{\lambda}(z)$ its d.c. term. We take the sign (+) if $u=y$, and the sign (−) if $u=x$.

One often finds the above expression written as:

$$F_u = \frac{e}{\pi \ \varepsilon_0} \left[\frac{1}{\gamma^2} \left(\frac{\varepsilon_0}{a^2} \mp \frac{\varepsilon_1}{h^2} \right) \lambda \mp \beta^2 \left(\frac{\varepsilon_1}{h^2} + \frac{\varepsilon_2}{g^2} \right) \bar{\lambda} \right] u \tag{56}$$

where the Laslett form factors [10] ε_0, ε_1 and ε_2 can be obtained for several beam pipe geometries. For example, for parallel plates, by comparing eq. (55) with (56) we get $\varepsilon_0 = 1/2$, $\varepsilon_1 = \pi^2/48$, $\varepsilon_2 = \pi^2/24$ [11]. It is interesting to note that these forces are anyway linear in the transverse displacement x and y.

3.8 Longitudinal direct space charge force

Up to now we have obtained the transverse forces, direct and indirect, produced by space charge distributions. The longitudinal electric field, responsible of the longitudinal forces, can be derived

starting from the knowledge of the transverse fields, as shown in Appendix 2. The transverse electric field inside the beam ($r \leq a$) can be expressed by the first of eqs. (32) for a uniform transverse distribution, which however can be generalized by considering a non uniform longitudinal distribution $\lambda(z)$, and outside the beam $r \geq a$ it is equal to

$$E_r(r \geq a) = \frac{\lambda(z)}{2\pi\varepsilon_0 r} \tag{57}$$

As a consequence the last equation of the Appendix 2 becomes

$$E_z(r,z) = -\frac{1}{2\pi\varepsilon_0\gamma^2}\left[\int_r^a \frac{r'}{a^2}dr' + \int_a^b \frac{1}{r'}dr'\right]\frac{\partial\lambda(z)}{\partial z} \tag{58}$$

giving a longitudinal force of the kind

$$F_z(r,z) = \frac{-e}{4\pi\varepsilon_0\gamma^2}\left(1 - \frac{r^2}{a^2} + 2\ln\frac{b}{a}\right)\frac{\partial\,\lambda(z)}{\partial\,z} \tag{59}$$

Therefore, the longitudinal force acting on a charge is positive (negative) in the region with negative (positive) density slope.

4.   Coherent and incoherent tune shifts

4.1   Coherent and incoherent effects

We are now ready to study the effects of the space charge forces on the beam dynamics. When the beam is located at the centre of symmetry of the pipe, the e.m. forces due to direct space charge and images cannot affect the motion of the centre of mass (coherent motion), but they change the trajectory of individual charges inside the beam (incoherent effects). These forces may have a complicate dependence on the charge position. A simple analysis is done considering only the linear expansion of the self induced forces around the equilibrium trajectory, as the forces given by eq. (34) or (55).

Referring to the equations of motion (22), (23), and (28), we now focus our attention to the self induced forces and expand them around the ideal orbit analogously to what we have done for the external forces. A constant term in the expansion of F^{self} changes the equilibrium orbit in the transverse plane, and the synchronous phase in the longitudinal one, while the linear term, proportional to the displacement, changes the focusing strength and therefore induces a shift of the betatron and synchrotron frequencies.

This can happen either in the motion of individual particles inside the beam (incoherent motion), and in the transverse oscillations of the whole beam (coherent motion) around the closed orbit when the beam is off-center with respect to the beam pipe.

4.2   Transverse incoherent effects

Let us consider only the linear term of the transverse self induced forces, that is

$$F_x^{self}(x,s) \cong \left(\frac{\partial F_x^{self}}{\partial x}\right)_{x=0} x \tag{60}$$

In case of uniform transverse beam distribution, either in a circular pipe and between parallel plates, the force given by eq. (60) is not an approximation, as shown by eqs. (34) and (55). For other kind of distributions, as the one given by eq. (35), we can always suppose that the transverse displacement r of a charge is much smaller than the transverse bunch dimension σ_r, so that the term inside the square brackets in eq. (37) can be expanded at first order in r giving $r/(2\sigma_r)$. In any case we end up with a self induced force linearly dependent on the particle displacement. As a consequence, by considering, for example, the motion along the x direction, eq. (22) becomes

$$x''(s) + \left(\frac{Q_x}{\rho_x}\right)^2 x(s) = \frac{1}{m_0 v_z^2 \gamma}\left(\frac{\partial F_x^{self}}{\partial x}\right)_{x=0} x(s) \tag{61}$$

The linear additional term on the right hand side produces a shift of the betatron tune Q_x. Indeed we can write

$$x''(s) + \left[\left(\frac{Q_x}{\rho_x}\right)^2 - \frac{1}{\beta^2 E_0}\left(\frac{\partial F_x^{self}}{\partial x}\right)_{x=0}\right] x(s) = 0 \tag{62}$$

where the term $m_0 v_z^2 \gamma$ has been substituted with $\beta^2 E_0$. We now recognize in the brackets a term proportional to the square of the new betatron tune, shifted, with respect to the initial one Q_x, by the self induced forces. This term can be written as $(Q_x + \Delta Q_x)^2 / \rho_x^2$. For small perturbations, the shift ΔQ_x can then be obtained by:

$$\left[\left(\frac{Q_x}{\rho_x}\right)^2 - \frac{1}{\beta^2 E_0}\left(\frac{\partial F_x^{self}}{\partial x}\right)_{x=0}\right] = \frac{(Q_x + \Delta Q_x)^2}{\rho_x^2} \cong \frac{Q_x^2 + 2Q_x \Delta Q_x}{\rho_x^2} \tag{63}$$

thus giving

$$\Delta Q_x = -\frac{\rho_x^2}{2\beta^2 E_0 Q_x}\left(\frac{\partial F_x^{self}}{\partial x}\right) \tag{64}$$

A similar expression is found in the y direction. The betatron tune shift is negative since the space charge forces are defocusing on both planes. Notice that the tune shift is in general function of z, due to the dependence of the self induced force on $\lambda(z)$. The consequence is a tune spread inside the beam. This conclusion is generally true also for more realistic non-uniform transverse beam distributions, which are characterized by a tune shift dependent also on the betatron oscillation amplitude. In these cases, instead of tune shift the effect is called tune spread.

As example of application of the above expression, let's find the incoherent shift of the betatron tune for a uniform electron beam of charge eN_p, radius a and length l_0, inside a circular pipe. The self induced force is given by eq. (34), with $\lambda(z) = eN_p / l_0$ so that

$$\Delta Q_x = -\frac{\rho_x^2 e^2 N_p}{4\pi\varepsilon_0 a^2 l_0 \beta^2 \gamma^2 E_0 Q_x} \tag{65}$$

or, expressed in terms of the classical radius of electron r_0:

$$\Delta Q_x = -\frac{r_0 \rho_x^2 N_p}{a^2 l_0 \beta^2 \gamma^3 Q_x} \tag{66}$$

In the general case of non-uniform focusing along the accelerator, as given by eq. (16), the linear effect of the self induced forces can be treated as a quadrupole error ΔK_u [11] distributed along the accelerator, with u representing one of the axis x or y, thus giving a betatron tune shift of:

$$\Delta Q_u = \frac{1}{4\pi}\oint \beta_u(s)\Delta K_u(s)ds = \frac{-1}{4\pi\beta^2 E_0}\oint \beta_u(s)\left(\frac{\partial F_u^{self}}{\partial u}\right)ds \tag{67}$$

For example, by considering the previous case of a uniform electron beam inside a circular pipe, but with non-uniform focusing, eq. (65) will be replaced by

$$\Delta Q_x = -\frac{r_0 N_p}{2\pi\beta^2\gamma^3 l_0}\oint \frac{\beta_x(s)}{a^2(s)}ds = -\frac{r_0 N_p}{2\pi\beta^2\gamma^3 l_0}\frac{2\pi\rho_x}{\varepsilon_x} \tag{68}$$

which has been obtained by observing that the quantity $a^2(s)/\beta(s)$ is the beam emittance ε_x, which is constant along the machine.

4.3   Transverse coherent effects

Let us suppose to have a beam displaced from the pipe axis, due for example to coherent betatron oscillations. Due to induction, there will be a higher concentration of charges of opposite sign on the pipe surface closer to beam, which attracts the beam itself more intensely than the induced charges on the opposite side. As a consequence, its center of mass will experience a defocusing force.

As example, let us suppose to have an electron beam with uniform longitudinal charge distribution $\lambda_0 = eN_p/l_0$ inside a conducting cylindrical pipe of radius b, displaced by x from its axis, as shown in Fig. 8. Since the electric field lines of the charge distribution must be perpendicular to the pipe, by imposing that the conductor surface is equipotential, we can remove and substitute the pipe with a charge distribution $-\lambda_0$ at a distance on the axis equal to $d=b^2/x$ on the same direction of the displacement.
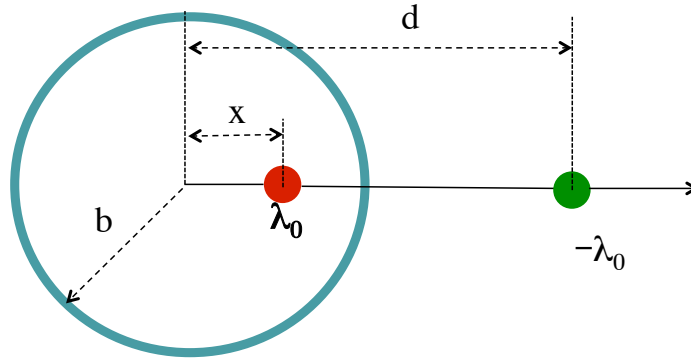

Fig. 8: A charge distribution inside a cylindrical pipe and its image charge distribution.

The image charge distribution attracts the whole beam thus producing a coherent defocusing effect. The electric field of the image charge acting on the center of mass of the beam is

$$E_x^{im}(x) \cong \frac{\lambda_0}{2\pi\ \varepsilon_0}\frac{1}{d-x} \tag{69}$$

If we linearize the electric field by considering small displacements of the beam, such that $x<<d$, then $1/(d-x) \cong 1/d = x/b^2$, and we obtain

$$E_x^{im}(x) \cong \frac{\lambda_0}{2\pi \, \varepsilon_0} \frac{x}{b^2} \qquad (70)$$

which gives a linear coherent force

$$F_x^{self}(x) \cong \frac{e\lambda_0}{2\pi \, \varepsilon_0} \frac{x}{b^2} \qquad (71)$$

This force produces a coherent betatron tune shift that can still be evaluated by using eq. (64) giving

$$\Delta Q_x = -\frac{\rho_x^2 e\lambda_0}{4\pi \, \varepsilon_0 \beta^2 E_0 b^2 Q_x} = -\frac{r_0 \rho_x^2 N_p}{b^2 l_0 \beta^2 \gamma Q_x} \qquad (72)$$

This coherent betatron tune shift, differently from the incoherent one given by eq. (66), does not depend on the beam size but on the pipe radius and it is inversely proportional to the beam energy.

4.4 Longitudinal incoherent effects

The effects of longitudinal space charge forces on the beam dynamics can be obtained by using eq. (28). We expand the self induced force and, as already discussed in section 4.1, we observe that the constant term in the expansion leads to a shift of the synchronous phase, while the linear term, proportional to the displacement, changes the focusing strength and therefore induces a shift of the synchrotron tune.

Let us analyse the motion of the beam around the new equilibrium phase and let us consider the linear term of the longitudinal self induced force:

$$F_z^{self}(r,z) \cong \left(\frac{\partial F_z^{self}}{\partial z}\right)_{z=0} z \qquad (73)$$

The equation of motion (28) becomes

$$z'' + \left(\frac{Q_z}{\rho_x}\right)^2 z = \frac{\eta}{\beta^2 E_0}\left(\frac{\partial F_z^{self}}{\partial z}\right)_{z=0} z \qquad (74)$$

As in the transverse case, let us consider the same approximation leading to eq. (63), obtaining in this case

$$\Delta Q_z = \frac{-\eta \rho_x^2}{2\beta^2 E_0 Q_z}\left(\frac{\partial \, F_z^{self}}{\partial z}\right) \qquad (75)$$

Differently from the transverse betatron tune shifts, the synchrotron tune shift can be either positive or negative and changes with the position of the charge inside the beam.

For example let us consider a transverse uniform beam of radius a in a cylindrical pipe, having a parabolic longitudinal distribution of the kind

$$\lambda(z) = \frac{3eN_p}{2l_0}\left[1 - \left(\frac{2z}{l_0}\right)^2\right] \qquad (76)$$

The incoherent tune shift can be obtained by combining eqs. (59), (75) and (76), thus giving

$$\Delta Q_z = -6 \frac{\eta \rho_x^2 r_0 N_p}{\beta^2 \gamma^3 Q_z} \left(1 - \frac{r^2}{a^2} + 2\ln\frac{b}{a}\right)\left(\frac{1}{l_0^3}\right) \tag{77}$$

which depends on the transverse position r of the charge inside the beam. If, instead of a parabolic bunch distribution, we had a Gaussian one, then the synchrotron tune shift would have a dependence also on the longitudinal position z.

5. Consequences of the space charge tune shifts

In circular accelerators the values of the betatron tunes should not be close to rational numbers in order to avoid the crossing of linear and non-linear resonances where the beam becomes unstable. The tune spread induced by the space charge force can make hard to satisfy this basic requirement. Typically, in order to avoid major resonances the stability requires [9, 12]

$$\left|\Delta Q_u\right| < 0.5$$

If the tune spread exceeds this limit, it is possible to reduce the effect of space charge tune spread by increasing the injection energy.

It is worth noting that the incoherent tune spread produces also a beneficial effect, called Landau damping, which can cure the coherent instabilities, provided that the coherent tune remains inside the incoherent spread.

6. Direct space charge effects in a Linac

In a Linac or a beam transport line direct space charge effects can lead to significant longitudinal-transverse correlations of the bunch parameters which may produce mismatch with the focusing and accelerating devices thus contributing to emittance growth (and energy spread). Matching conditions suitable to preserve the beam quality can be derived from a simple model as will be shown hereafter. A more detailed discussion can be found in the many classical textbooks on this subject as the ones listed in references [3,13].

Let us consider a *bunched* beam with initially uniform charge distribution in a cylinder of radius R and length l_0, carrying a current I and moving with longitudinal velocity $v = \beta c$. The linear components of the longitudinal and transverse space charge fields are given by [14]:

$$E_z(\zeta) = \frac{IL}{2\pi\varepsilon_0 R^2 \beta c} h(\zeta) \tag{78}$$

$$E_r(r,\zeta) = \frac{Ir}{2\pi\varepsilon_0 R^2 \beta c} g(\zeta) \tag{79}$$

where the field form factors are described by the functions:

$$h(\zeta) = \sqrt{A + (1-\zeta)^2} - \sqrt{A + \zeta^2} + (2\zeta - 1) \tag{80}$$

$$g(\zeta) = \frac{(1-\zeta)}{2\sqrt{A^2 + (1-\zeta)^2}} + \frac{\zeta}{2\sqrt{A^2 + \zeta^2}} \tag{81}$$

where $\zeta = \dfrac{z}{L}$ is the normalized longitudinal coordinate along the bunch and $A = \dfrac{R}{\gamma L}$ is the beam aspect ratio. As γ increases $g(\zeta) \to 1$ and $h(\zeta) \to 0$. Thus, direct space charge fields mainly affect transverse beam dynamics.

The transverse beam dynamics of a beam characterized by an rms envelope $\sigma = \sqrt{\langle x^2 \rangle}$ and transverse normalized thermal rms emittance at the source [3]:

$$\varepsilon_{n,th}^2 = \frac{\langle x^2 \rangle \langle p_x^2 \rangle}{(m_o c)^2} = \frac{\gamma k_B T \sigma_o^2}{m_o c^2} \tag{82}$$

can be conveniently described, under the paraxial ray approximation, i. e. $p_x \ll p_z$, by the rms envelope equation that for an axisymmetric beam is [3,15,16]:

$$\sigma'' + \frac{\gamma'}{\gamma}\sigma' + k_{ext}^2 \sigma = \frac{K_{sc}}{\gamma^3 \sigma} + \frac{\varepsilon_{n,th}^2}{\gamma^2 \sigma^3} \tag{83}$$

The first term is the change in the envelope slope, the second term drives the envelope oscillation damping due to acceleration, the third term accounts for linear external focusing forces, the fourth represents the defocusing space charge effects and the fifth the internal pressure due to the emittance. $K_{sc} = \dfrac{\hat{I}}{2 I_A}$ is the *beam perveance*, $\hat{I}$ is the peak current, I_A the Alfvén current (~17 kA), and $\gamma' = \dfrac{e E_{acc}}{mc^2}$, E_{acc} being the accelerating field.

From the envelope equation (83) we can identify two regimes of beam propagation: *space charge dominated* and *emittance dominated*. A beam is space charge dominated as long as the space charge collective forces are largely dominant over the emittance pressure. A measure of the relative importance of space charge effects versus emittance pressure is given by the *laminarity parameter*, defined as the ratio between the space charge term and the emittance term:

$$\rho = \frac{\hat{I}}{2 I_A \gamma} \frac{\sigma^2}{\varepsilon_n^2} \tag{84}$$

When ρ greatly exceeds unity, the beam behaves like a laminar flow (all beam particles move on trajectories that do not cross) and transport and acceleration require a careful tuning of focusing and accelerating elements in order to keep laminarity. Correletated emittance growth is typical in this regime which can be conveniently made reversible if proper beam matching conditions are fulfilled, as discussed hereafter. When $\rho < 1$ the beam is emittance dominated (also named thermal regime corresponding to a Debye length large compare to the bunch envelope) and the space charge effects can be neglected. The transition to thermal regime occurs when $\rho \approx 1$ corresponding to the transition energy

$$\gamma_{tr} = \frac{\hat{I}}{2 I_A} \frac{\sigma^2}{\varepsilon_n^2} \tag{85}$$

For example a beam with $\hat{I}$=100 A, ε_n=1 μm, and σ=300 μm is leaving the space charge dominated regime and is entering the thermal regime at the transition energy of 131 MeV. From this example one may conclude that space charge dominated regime is typical of low energy beams. Actually for applications like linac driven Free Electron Lasers high density beams with peak currents exceeding kA are required. Even if the bunch energy has reached values higher than γ_{tr}, space charge effects may recur if bunch compressors are active increasing $\hat{I}$, so that a new transition energy with higher $\hat{I}$ has to be considered.

When longitudinal correlations within the bunch are important, as the one induced by the space charge effects, the beam envelope evolution is generally dependent also on the longitudinal bunch coordinate ζ. In this case the bunch should be considered as an ensemble of N longitudinal slices of envelope $\sigma_s(z,\zeta)$ whose evolution can be computed considering N slice envelope equations equivalent to (83) provided that the bunch parameters refer to each single slice: γ_s, γ'_s, $k_{sc,s} = k_{sc}g(\zeta)$. Correlations within the bunch may cause emittance oscillations that can be evaluated, once a solution of the slice envelope equation is known, by using the following correlated emittance definition:

$$\varepsilon_{n,rms,cor} = \langle\gamma\rangle\sqrt{\langle\sigma_s^2\rangle\langle\sigma_s'^2\rangle - \langle\sigma_s\sigma_s'\rangle}$$ (86)

where the average is performed over the entire slice ensemble. In the simplest case of only 2 slices the previous definition reduces to:

$$\varepsilon_{n,rms,cor} = \langle\gamma\rangle|\sigma_1\sigma_2' - \sigma_2\sigma_1'|$$ (87)

which is a simple and useful formula for an estimation of the emittance scaling [17].

The total normalized rms emittance is then given by the superposition of the correlated and uncorrelated terms as :

$$\varepsilon_{n,rms} = \sqrt{\varepsilon_{n,th}^2 + \varepsilon_{n,rms,cor}^2}$$ (88)
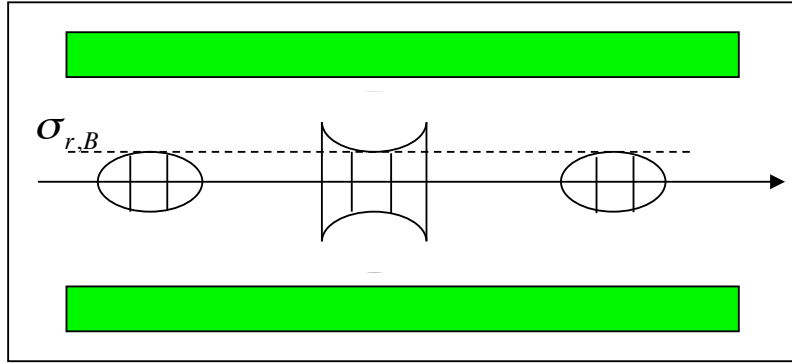

Fig. 9 - Schematic representation of a nearly matched beam in a long solenoid. The dashed line represent the reference slice envelope fully matched to the Brillouin flow condition. The other slice envelopes are oscillating around the equilibrium solution.

An interesting example [6] to consider here, showing the consequences of a non perfect beam matching, is the propagation of a beam in the space charge dominated regime nearly matched to an external focusing channel produced by a long solenoid, giving $k_{ext}^2 = k_{sol}^2 = \left(\dfrac{qB}{2\gamma m_o c}\right)^2$, as illustrated in Fig. 9. To simplify our analysis we can neglect acceleration, as in the case of a simple beam transport line. The envelope equation for each slice, indicated as σ_s, reduces to:

$$\sigma_s'' + k_{ext}^2\sigma_s = \frac{k_{sc,s}}{\gamma^3\sigma_s}$$ (89)

A stationary solution, called *Brillouin flow*, is given by:

$$\sigma_{s,B} = \frac{1}{k_{ext}^2}\sqrt{\frac{\hat{I}g(\zeta)}{2\gamma^3 I_A}}$$ (90)

where the local dependence of the current $\hat{I}_s = \hat{I}g(\varsigma)$ within the bunch has been explicitly indicated. This solution represents the matching conditions for which the external focusing completely balances the internal space charge force. Unfortunately since k_{ext} has a slice independent constant value, the Brillouin matching condition cannot be achieved at the same time for all the bunch slices. Assuming there is a reference slice perfectly matched with an envelope $\sigma_{r,B}$, the matching condition for the other slices can be written as:

$$\sigma_{sB} = \sigma_{rB} + \frac{\sigma_{rB}}{2}\left(\frac{\delta I_s}{\hat{I}}\right) \tag{91}$$

with respect to the reference slice. Considering a small perturbation δ_s from the equilibrium in the form

$$\sigma_s = \sigma_{s,B} + \delta_s \tag{92}$$

and substituting in the equation (89) we can obtain a linearized equation for the slice offset:

$$\delta_s'' + 2k_{ext}^2\delta_s = 0 \tag{93}$$

which has a solution given by:

$$\delta_s = \delta_o \cos\left(\sqrt{2}k_{ext}z\right) \tag{94}$$

where $\delta_o = \sigma_{so} - \sigma_{sB}$ is the amplitude of the initial slice mismatch that we assume for convenience the same for all slices. Inserting (94) in (92) we get the perturbed solution:

$$\sigma_s = \sigma_{s,B} + \delta_o \cos\left(\sqrt{2}k_{ext}z\right) \tag{95}$$

Equation (95) shows that slice envelopes oscillate altogether around the equilibrium solution with the same frequency for all slices ($\sqrt{2}k_{ext}$, often called plasma frequency) dependent only on the external focusing forces. This solution represents a collective behavior of the bunch similar to the one of the electrons subject to the restoring force of ions in a plasma. Using the two slices model and eq. (95) the emittance evolution (87) results:

$$\varepsilon_{n,rms,cor} = \frac{1}{4}\langle\gamma\rangle k_{ext}\sigma_{r,B}\left|\frac{\Delta I}{\hat{I}}\delta_o \sin\left(\sqrt{2}k_{ext}z\right)\right| \tag{96}$$

where $\Delta I = \hat{I}_1 - \hat{I}_2$. Notice that in this simple case envelope oscillations of the mismatched slices induce correlated emittance oscillations which periodically goes back to zero, showing the reversible nature of the correlated emittance growth. It is, in fact, the coupling between transverse and longitudinal motion induced by the space charge fields that allows reversibility. With a proper tuning of the transport line length or of the focusing field one can compensate for the transverse emittance growth. Similar arguments can be considered when including acceleration, despite the analytical treatment results to be more complex [6]. In this case for a well matched beam to the accelerating structure the plasma frequency $\sqrt{2}K_{ext} \to 0$ with increasing γ. Before the transition energy is

achieved, the emittance performs damped oscillations. A careful tuning of the external fields can minimize the value of the emittance at the beam extraction.

References

[1] K. Schindl, Space Charge, CAS Loutraki Greece 2000, CERN-2005-004 p. 285.

[2] L. Palumbo, V. G. Vaccaro, and M. Zobov, CERN 95-06, 1995, pp. 331–390.

[3] M. Reiser, "Theory and Design of Charged Particle Beams" , Wiley, New York, 1994

[4] A. Piwinski, in Proc. of the 9th Int. Conf. on High Energy Accelerators, Stanford, CA, 1974

[5] C. Bernardini et al., Phys. Rev. Lett. 10, 407–409 (1963)

[6] L. Serafini, J.B. Rosenzweig, Phys. Rev. E 55, 7565 (1997)

[7] F. F. Chen, "Introduction to plasma physics and controlled fusion", Vol. 1, Springer 1974.

[8] R. Davidson, "Physics of non-neutral plasmas", Addison Wesley, 1990.

[9] J. Rossbach, P. Schmüser, 'Basic course on accelerator optics', CAS Jyväskylä 1992, CERN 94–01, p. 76.

[10] L. J. Laslett, "Selected Works of L. J. Laslett", Vol. III, LBL-PUB-616, September 1987.

[11] See, e.g. 'Handbook of Accelerator Physics and Engineering" edited by A. W. Chao and M. Tigner, World Scientific, p. 114.

[12] J. P. Delahaye, et al., Proc. 11th Int. Conf. on High Energy Accelerators, Geneva, 1980, p. 299.

[13] A. W. Chao, Physics of Collective Beam Instabilities in High Energy Accelerators (John Wiley & Sons, New York, 1993), p. 14.

[14] M. Ferrario et al., Int. Journal of Modern Physics A, Vol 22, No. 23, 4214 (2007).

[15] J. B. Rosenzweig, "Fundamentals of beam physics", Oxford University Press, New York, 2003

[16] M. Ferrario, "Accelerator physics: basic principles on beam focusing and transport", Proc. of the Int. School of Physics "Enrico Fermi", Course CLXXIX - "Laser-Plasma Acceleration" – Varenna - 20 - 25 June 2011, Ed. By F. Ferroni, L. Gizzi and R. Faccini, Societa' Italiana di Fisica.

[17] J. Buon, "Beam phase space and emittance", in CERN 94-01

APPENDIX 1 – BOUNDARY RELATIONS FOR CONDUCTORS

A1.1 STATIC ELECTRIC AND MAGNETIC FIELDS

When we have two materials with different relative permittivity, which we call ε_{r1} and ε_{r2}, in the passage from one material to another, the tangential electric field and the normal electric displacement are preserved, so that we have the boundary relations:

$$E_{t1} = E_{t2}$$
$$\varepsilon_{r1}E_{n1} = \varepsilon_{r2}E_{n2}$$

If one of the two materials is a conductor with a finite conductivity, then the electric field vanishes inside it, and the walls are equipotential surfaces. This implies that the electric field lines are orthogonal to the conductor surface, independently of the dielectric and magnetic properties of the material. The only condition is to have a finite conductivity.

If we have a charge close to a conductor, in order to obtain the electric field, we need to include the effects of the induced charges on the conducting surfaces, and we must know how they are distributed. Generally this task is not easy, but if we have an infinite conducting screen, the problem can be easily solved by making use of the method of images: we can remove the screen and put at a symmetric location a charge with opposite sign, as shown in Fig. A1.
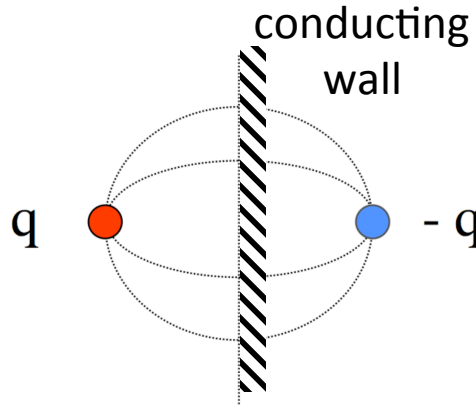

Fig. A1: Method of images.

The total electric field is the sum of the direct and the image field:

$$\vec{E}^{tot} = \vec{E}^{direct} + \vec{E}^{images}$$

For the static magnetic field between two materials with different permeability, the following boundary relations hold:

$$H_{t1} = H_{t2}$$
$$\mu_{r1}H_{n1} = \mu_{r2}H_{n2}$$

Thus, static magnetic fields do not perceive the presence of the conductor, if it has a magnetic permeability $\mu_r \approx 1$, as copper or aluminium, and the field lines expand as in the free space. However, a beam pipe in a real machine goes through many magnetic components (like dipoles and quadrupoles) made of ferromagnetic materials with high permeability (of the order of $10^3 - 10^5$). For these materials, due to the boundary conditions, the magnetic field lines are practically orthogonal to the surface. Similarly to electric field lines for a conductor, the total magnetic field can be derived by

using the image method: we remove the magnetic wall and put a symmetric current with same sign, as shown in Fig. A2.
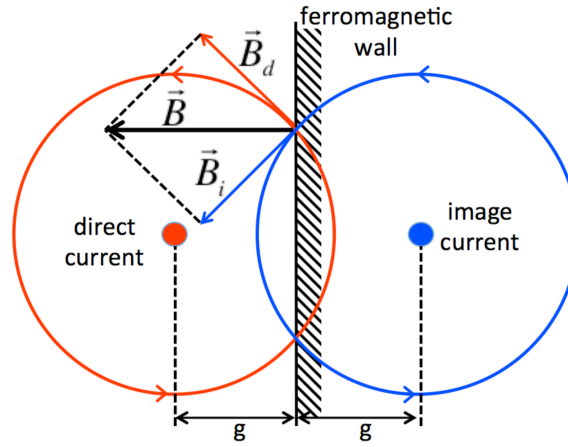

Fig. A2: Method of image current.

A1.2 TIME VARYING FIELDS

Static electric fields vanish inside a conductor for any finite conductivity, while static magnetic fields pass through unless of high permeability. This is no longer true for time changing fields, which can penetrate inside the material in a region δ_w called skin depth. In order to write the skin depth as a function of the material properties, we write the following Maxwell's equations inside the conducting material together with the constitutive relations:

$$\begin{cases} \nabla \times \vec{E} = -\dfrac{\partial \vec{B}}{\partial t} \\ \nabla \times \vec{H} = \vec{J} + \dfrac{\partial \vec{D}}{\partial t} \end{cases} \qquad \begin{cases} \vec{B} = \mu \vec{H} \\ \vec{D} = \varepsilon \vec{E} \\ \vec{J} = \sigma \vec{E} \end{cases}$$

Let us consider a plane wave linearly polarized with the electric field in the y direction propagating in the material along x, as shown in Fig. A3.
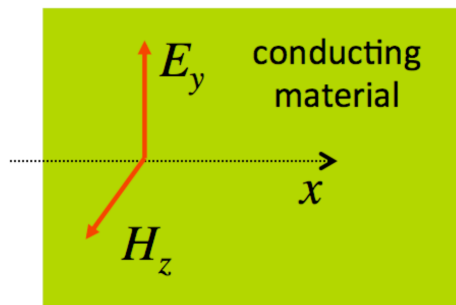

Fig. A3: Plane wave propagating inside a conducting material.

From the Maxwell's equations we get the wave equation for the electric field:

$$\frac{\partial^2 E_y}{\partial x^2} - \varepsilon\mu\frac{\partial^2 E_y}{\partial t^2} - \sigma\mu\frac{\partial E_y}{\partial t} = 0$$

In order to find the solution of the wave equation, we assume that the electric field propagates in the x direction with the law

$$E_y = \tilde{E}_0 e^{i\omega t - \gamma x}$$

If we substitute the above expression in the wave equation, we get the equation for the complex amplitude of the electric field $\tilde{E}_0$

$$(\gamma^2 + \varepsilon\mu\omega^2 - i\omega\mu\sigma)\tilde{E}_0 e^{i\omega t - \gamma x} = 0$$

An analogous equation holds for H_z. In order to have non-zero electric field, the term inside the parentheses must be zero. If σ>>ωε this reduces to

$$\gamma \cong (1+i)\sqrt{\frac{\sigma\mu\omega}{2}}$$

Under such a condition we say that the material behaves like a conductor. Since γ has a real part, fields propagating in the material are attenuated. The attenuation constant, measured in meters, is called skin depth δ_w:

$$\delta_w \cong \frac{1}{\Re(\gamma)} = \sqrt{\frac{2}{\omega\sigma\mu}}$$

The skin depth depends on the material properties and the frequency. Copper, for example, has a skin depth of

$$\delta_w \cong \frac{6.66}{\sqrt{f}}(cm)$$

If we assume a beam pipe 2 mm thick, we find that fields pass through the wall up to frequencies of 1 kHz.

Time varying fields generally pass through the conductor wall if the skin depth is larger than the wall thickness. This happens at relatively low frequency when δ_w is large, while at higher frequencies, for a good conductor, the skin depth is very small and much lower than the wall thickness, so that we can consider that both electric and magnetic fields vanish inside the wall. In this condition, the electric field lines are perpendicular to the wall surface, as in the static case, while the magnetic field lines are tangent to the wall. As a consequence, in order to obtain the electric field which is time varying close to a good conductor, we can still use the method of the images, while for the magnetic field it is easy to see that we can use the method shown in Fig. A2, by changing the direction of the image current.

APPENDIX 2 – LONGITUDINAL FORCES

In order to derive the relationship between the longitudinal and transverse forces inside a beam, let us consider the case of cylindrical symmetry and ultra-relativistic bunches. We know from Faraday's law of induction that a varying magnetic field produces a rotational electric field:

$$\oint \vec{E} \cdot d\vec{l} = -\frac{\partial}{\partial t} \int_S \vec{B} \cdot \hat{n}\, dS$$

In order to obtain the longitudinal electric field, we choose, as path for the circulation, a rectangle going through the beam pipe (a cylinder of radius b) and the beam, parallel to the z axis and with radius a, as shown in Fig. A4. For a generic position $r<a$, and by taking Δz small enough so that we can consider the electric field constant, we have:

$$E_z(r,z)\Delta z + \int_r^b E_r(r,z+\Delta z)dr - E_z(b,z)\Delta z - \int_r^b E_r(r,z)dr = -\Delta z \frac{\partial}{\partial t}\int_r^b B_\phi(r)dr$$

We now write $E_r(r,z+\Delta z) - E_r(r,z) = \dfrac{\partial E_r(r,z)}{\partial z}\Delta z$ so that from the above equation we get

$$E_z(r,z) = E_z(b,z) - \int_r^b \left[\frac{\partial E_r(r,z)}{\partial z} + \frac{\partial B_\phi(r,z)}{\partial t}\right]dr$$

By considering that $z = -\beta ct$, we can also write

$$E_z(r,z) = E_z(b,z) - \frac{\partial}{\partial z}\int_r^b \left[E_r(r,z) - \beta c B_\phi(r,z)\right]dr$$

Since the transverse electric field and the azimuthal magnetic field are related by $B_\phi = \dfrac{\beta}{c}E_r$, we finally obtain

$$E_z(r,z) = E_z(b,z) - \left(1-\beta^2\right)\frac{\partial}{\partial z}\int_r^b E_r(r,z)dr$$

Note that for perfectly conducting walls we have $E_z(b,z) = 0$, so that

$$E_z(r,z) = -\frac{1}{\gamma^2}\frac{\partial}{\partial z}\int_r^b E_r(r,z)dr$$
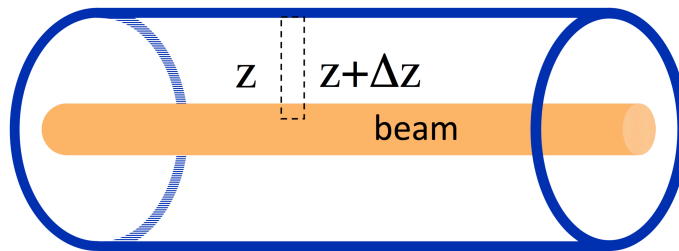

Fig. A4: Geometry for obtaining the longitudinal electric field due to space charge.